INTERNATIONAL JOURNAL OF
ENERGY AND ENVIRONMENT

Volume 1, Issue 6, 2010 pp.1027-1038
Journal homepage: www.IJEE.IEEFoundation.org

Heat transfer enhancement of free surface MHD-flow by the wall with non-uniform electrical conductivity

H. L. Huang, B. Li

Academy of Frontier Science, Nanjing University of Aeronautics and Astronautics, Nanjing, 210016, P.R.China.

Abstract
Due to the Magnetohydrodynamic (MHD) effect, which degrades heat transfer coefficients by pulsation suppression of external magnetic field, on the electrically conducting flow, the wall with non-uniform electrical conductivity is employed in a free surface MHD-flow system for heat transfer enhancement. The non-uniform electrical conductivity distribution of the channel wall may create alternate Lorentz forces along spanwise direction, which can effectively produce flow disturbance, promote mixture, reduce the thickness of boundary layer, and enhance heat transfer. So the heat transfer performances enhanced by some conducting strips aligned with the mean flow direction on the insulating wall of free surface MHD-flow are simulated numerically in this paper. The flow behaviors, heat transfer coefficients, friction factors and pressure drops are presented under different Hartmann numbers. Results show that, in the range of Hartmann numbers $30 \leq Ha \leq 100$, the wall with non-uniform conductivity can achieve heat transfer enhancements (Nu/Nu_0) of about 1.2 to 1.6 relative to the insulating wall, with negligible friction augmentation. This research indicates that the modules with three or five conducting strips can obtain better enhancement effect in our research. Particularly, the heat transfer augmentation increases monotonically with increasing Hartmann numbers. Therefore, the enhancement purpose for high Hartman number MHD-flow is marked, which may remedy the depressing heat transfer coefficients by MHD effect.

Keywords: Heat transfer enhancement, Non-uniform electrical conductivity, Free surface, Magnetohydrodynamic, MHD-flow.

1. Introduction

The motion of electrically conducting fluid in a strong magnetic field generally induces electric currents, which interact with the magnetic field and generate electromagnetic forces that change the velocity distribution and turbulent pulsation characteristics and exhibit an integral retarding force on the flow. These effects change heat transfer performances, friction factor, pressure drop, and the required pumping power of the system in comparison with those of the cases without magnetic field. The external magnetic field suppresses turbulent pulsations even if it is not enough to substantially influence the average velocity profile, which leads in general to a decrease of heat transfer coefficient (Nusselt number Nu) with the increase of magnetic fields. For many engineering applications, such as the first wall in fusion engineering, the heat transfer performance has to be improved to extract heat energy and reduce the

friction loss as much as possible. Then, heat transfer enhancement methods which maximize heat transfer augmentation with minimal friction penalty are sought.

Recently, various surface topologies have been used to increase the disturbance in the fluids and enhance convective heat transfer in some engineering applications for MHD flow, as in metallurgical processes, continuous casting and the first wall design of fusion blanket [1]. These surface topologies, such as pin-fin array and ribs, have an additional aspect, i.e. any design has to be sensitive to the friction penalty of achieving heat transfer enhancement. Meanwhile, a number of investigations have indicated that the enhancement purpose for high Hartman number MHD flow is not marked [1, 2].

Buehler [3] provided computational results of the instabilities in quasi-two-dimensional MHD flow, in which the walls contained a conducting strip aligned with the mean flow direction. In his study, the main flow exhibited wake-character with the vortex street developing in the downstream. However, no attention has been paid to enhancing the heat transfer of the MHD flow by the non-uniform electrical conductivity wall at present.

The objective of this paper is to investigate the heat transfer performance enhanced by the wall with non-uniform electrical conductivity for free surface MHD-flow. Through the numerical analysis, the flow behaviors, heat transfer coefficients, friction factors and pressure drops are presented under different Hartmann numbers.

2. Physical and mathematical models

Figure 1 shows the domain of computational model. The configuration consists of a rectangular open channel containing several conducting strips of conductance at the bottom wall, aligned with the mean flow direction. The geometry scales are from Nygrena et.al. [2], where the channel width is d=0.027m, which is selected as characteristic length. The dimensionless length of the channel is L=3.7. The liquid metal (Re=11650, Re_m=14.3, Pr=0.05) flows through the open channel with uniform dimensionless thickness H=0.185 at the inlet, and the fluid above the liquid metal is taken as air. The applied external magnetic field is z direction, normal to the bottom wall. The dimensionless width of each conducting strip is S=0.1, and the number of conducting strips is m.

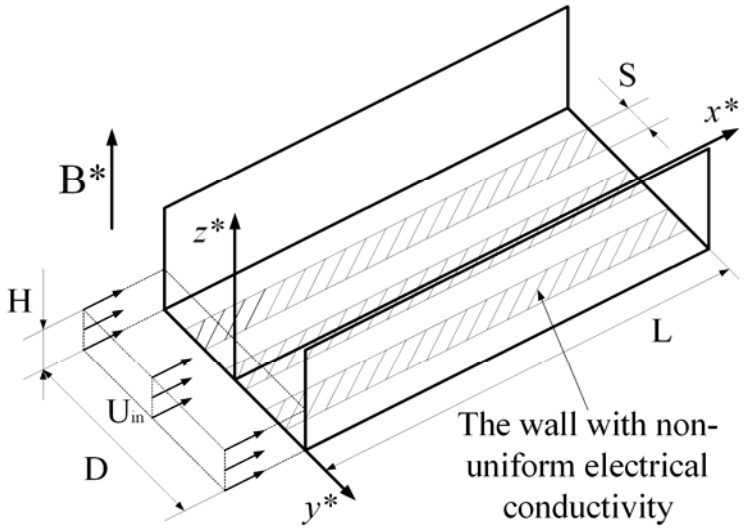

Figure 1. Schematic of the physical model

The dimensionless variables based on the channel width d and the velocity at the inlet U_{in} are as follow:

$$\left(x^*, y^*, z^*\right)=\left(\frac{x}{d}, \frac{y}{d}, \frac{z}{d}\right),\ t^*=\frac{tU_{in}}{d},\ T^*=\frac{T-T_i}{T_w-T_i},\ \mathbf{V}^*=\frac{\mathbf{V}}{U_{in}},\ p^*=\frac{p}{\rho U_{in}^2},\ k^*=\frac{k}{U_{in}^2},\ \varepsilon^*=\frac{\varepsilon d}{U_{in}^2},$$

$$\boldsymbol{B}^*=\frac{\boldsymbol{B}}{B_0},\quad \mathbf{J}^*=\frac{\mathbf{J}}{\sigma_m U_{in} B_0},\quad \mu_t^*=Re\cdot C_\mu \frac{k^{*2}}{\varepsilon^*}\left[1-exp\left(-C_3 y^{+*}\right)\right],\quad y^{+*}=\sqrt{Re}\sqrt{\frac{\partial V^*}{\partial y^*}}y^*$$

The flow of an electrically conducting fluid under the influence of an external magnetic field is governed by the following dimensionless momentum equation:

$$\frac{\partial \mathbf{V}^*}{\partial t^*}+\left(\mathbf{V}^*\cdot\nabla\right)\mathbf{V}^*=-\nabla p^*+\nabla\cdot\left(\left(\frac{1}{\mathrm{Re}}+\mu_t^*\right)\nabla\mathbf{V}^*\right)+\frac{1}{Fr}+\frac{k\mathbf{n}\delta(\phi)}{We}+\frac{Ha^2}{\mathrm{Re}}\left(\mathbf{J}^*\times\mathbf{B}^*\right) \tag{1}$$

where $\delta(\phi)=|\nabla\phi|$ is the surface delta function, and ϕ is volume fraction. $\mathbf{B}^*$ is magnetic field intensity, including both the applied ($\mathbf{B}_0^*$) and induced magnetic field b*; $\mathbf{J}^*$ is induced current density, which can be gotten by

$$\mathbf{J}^*=\frac{1}{\mathrm{Re}_m}\left(\nabla\times b^*\right) \tag{2}$$

The induced magnetic field b* may be derived from Maxwell's equations and Ohm's law for uniform external magnetic field:

$$\frac{\partial \mathbf{b}^*}{\partial t}+\left(\mathbf{V}\cdot\nabla\right)\mathbf{b}^*=\nabla\cdot\left(\frac{1}{\mathrm{Re}_m}\nabla\mathbf{b}^*\right)+\left(\mathbf{B}^*\cdot\nabla\right)\mathbf{V}^* \tag{3}$$

Turbulence properties are calculated by considering the k−ε turbulence model governed by transport equations. The influences of magnetic fields on turbulence are realized in two ways. First, magnetic fields influence on the redistribution of turbulence and, the second, magnetic fields have an effect on the dissipation of turbulence. The transport equations for the turbulent kinetic energy, κ*, and the dissipation rate of the turbulent kinetic energy, ε*, have been derived for liquid metal flow, including the additional MHD effects based on the Reynolds' analogy for low magnetic Reynolds number, from Smolentsev et.al [4], Kitamura and Hirata [5].

$$\frac{\partial k^*}{\partial t^*}+\left(\mathbf{V}^*\cdot\nabla\right)k^*=\nabla\cdot\left((\mu^*+\frac{\mu_t^*}{\sigma_k})\nabla k^*\right)+\mu_t^*\nabla^2\mathbf{V}^*+\frac{\varepsilon^*}{\mathrm{Re}}-\frac{1}{\mathrm{Re}}\frac{2k^*}{x_2^{*2}}-C_3\frac{Ha^2}{\mathrm{Re}}k^* \tag{5}$$

$$\frac{\partial \varepsilon^*}{\partial t^*}+\left(\mathbf{V}^*\cdot\nabla\right)\varepsilon^*=\nabla\cdot\left((\mu^*+\frac{\mu_t^*}{\sigma_\varepsilon})\nabla\varepsilon^*\right)+C_1\frac{\varepsilon^*}{k^*}\mu_t^*\nabla^2\mathbf{V}^*-C_2\rho^*\frac{\varepsilon^{*2}}{k^*}-C_4\frac{Ha^2}{\mathrm{Re}}\varepsilon^* \tag{6}$$

where, C_1, C_2, and C_3 are constants chosen in accordance with Kitamura [5], σ_k and σ_ε are the turbulent Prandtl numbers for κ* and ε*, respectively. Here, C_3 and C_4 are adopted in the form of 1.9 e-^{2N}, 1.9e^{-4N}.

With the introduction of turbulent viscosity for heat transfer and the ignorance of the viscous heating, the energy equation is written as:

$$\frac{\partial T^*}{\partial t^*}+\left(\mathbf{V}^*\cdot\nabla\right)T^*=\frac{1}{Pe}\nabla\cdot\left[\left(1+\frac{\mu_t}{\sigma_t}\mathrm{Pr}\right)\nabla T^*\right] \tag{7}$$

where, $\sigma_t=0.7\times(1+\exp\{37\times(z^*/H-0.89)\})$ is turbulent Prandtl number, which stands for the ration between the eddy diffusivity for momentum and eddy diffusivity for heat and the value obtained from Smolentsev et.al [4].

2.1 Boundary conditions

A uniform velocity profile is employed at the inlet. An inlet turbulence intensity level of 1% is used, and the hydraulic diameter at the inlet is taken as equal to the width of the channel. According to experimental data on heat transfer in liquid metal MHD flow revealed in Nygrena et.al. [2], constant temperature boundary conditions are employed at the bottom wall at T_w^* =1 and the temperature of liquid metal is T_i^* = 0 at the channel inlet. Side walls are adiabatic, thus no heat is given to them. The

streamwise gradients of all variables such as velocity and temperature are set to zero at the outlet boundary to attain fully developed conditions.

2.2 Computational method

The grid is made up of hexahedral elements aligned with the flow direction to reduce the numerical diffusion errors and thus to improve the quality of the numerical predictions. Meshes of these regions near the wall and the interface are fined to resolve the typical high gradients. In the near-wall regions, enhanced wall treatment which combines a two-layer model with enhanced wall functions is utilized. The enhanced wall functions smoothly blend the law of an enhanced turbulent wall law with that of laminar wall law. So near-wall meshes are fully resolved for y+* values less than 1 to resolve the laminar sublayer. In order to check the grid convergence, simulations with six sets of different meshes are performed, and the concept GCI (grid convergence index) [6] is introduced. The average Nusselt number Nu_{av} [7], mean friction factor f_m and pressure drop ΔP are defined as monitors for each mesh. The grid convergence index $GCI(Nu_{av}) = |1 - Nu_{av}(Mi)/Nu_{av}(M6)|$, $GCI(f_m) = |1 - f_m(Mi)/f_m(M6)|$, and $GCI(\Delta P) = |1 - \Delta P(Mi)/\Delta P(M6)|$ are calculated. Shown in Table 1, the values of GCI(Nu_{av}), GCI(f_m) and GCI(ΔP) of M5 are all less than 2.7×10^{-3}, which indicate the grid M5 has good convergence. In order to save CPU time and keep a reasonable accuracy in our computations, all simulations are performed with the M5 mesh.

Table 1. Grid convergence index values under different meshes

Mesh	M1	M2	M3	M4	M5	M6
Number of nodes	0.8×10^5	1×10^5	1.2×10^5	1.4×10^5	2.2×10^5	4.2×10^5
GCI(f_m)	2.1×10^{-2}	1.1×10^{-2}	6.9×10^{-3}	3.4×10^{-3}	2.7×10^{-3}	0
GCI(ΔP)	5.6×10^{-2}	2.3×10^{-2}	8.9×10^{-3}	5.6×10^{-3}	1.3×10^{-3}	0
Nu_{av}	11.41	10.83	10.40	10.21	10.16	10.15
GCI(Nu_{av})	0.12	6.7×10^{-2}	2.4×10^{-2}	5.9×10^{-3}	9.8×10^{-4}	0

The Reynolds averaged Navier Stokes equations are solved numerically in conjunction with the turbulent transport equations and MHD equations. The discretization of the combined convective and diffusive fluxes across the control volumes is modeled by using the QUICK scheme. The pressure-velocity coupling is handled with the PISO scheme. The calculations are carried out on a non-uniform staggered grid system. The calculation domain involves free surfaces, thus the volume of fluid (VOF) method is adopted to capture its evolution.

2.3 Model validation

For the validation of this model, a calculation is conducted to compare with the numerical study of heat transfer in a free surface MHD flow by Smolentsev et.al [4]. Figure 2 summarizes the comparisons. The distributions of the turbulence kinetic energy show excellent agreement with Smolentsev's results. The maximum deviation detected is within a tolerable band of 10%.

3. Results and discussions

In order to investigate the heat transfer performance enhanced by the wall with non-uniform electrical conductivity for free surface MHD-flow, the flow behaviors, heat transfer coefficients, friction factors and pressure drops have been performed numerically. The effect of magnetic fields normal to bottom wall and corresponding with Hartmann number varying from 30 to 100, is investigated. Baseline Nusselt numbers Nu_0 and friction factors f_0 are measured with a uniform insulating wall replacing the non-uniform electrical conductivity wall at the same Hartmann numbers. These baseline values are used to normalize the uniform insulating wall values, and are thus used as a basis of comparison with non-uniform electrical conductivity wall values.

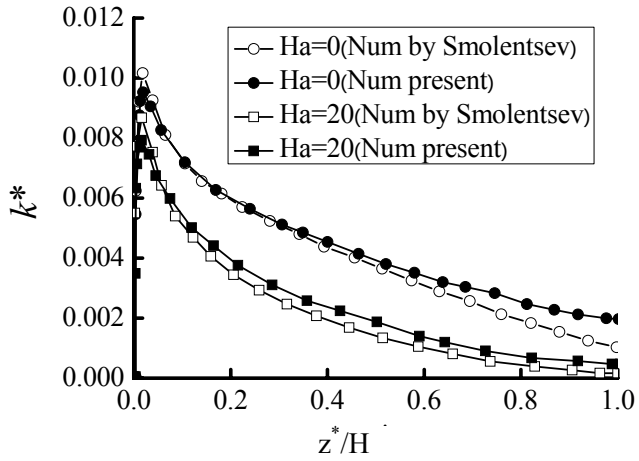

Figure 2. Comparison between numerical results and Smolentsev's results

The interaction of the moving fluid with the magnetic field induces an electric field $\mathbf{V}^* \times \mathbf{B}^*$ which drives the electric current J*. The electric conductivity of the channel walls influences the distribution of current in the fluid and determines the flow pattern. For a uniform insulating channel the electric currents distribution in the plane at x*=2.6 can be seen from Figure 3(a). Since no current can enter the wall, the currents induced in the bulk flow are blocked to go through the viscous boundary layers near the wall. However, as shown in Figure 3(b), several current circuits are formed in the transverse section plane under the influence of the wall with electrical conductivity strips. In the conducting strip regions, almost all currents enter the conductivity strips. In contrast, in the insulating wall regions, no currents can enter the wall and they cross through the viscous boundary layers near the wall. So the current direction in the vicinity of the conducting strip is opposite to that in the vicinity of the insulating wall, as is shown in Figure 3(b).

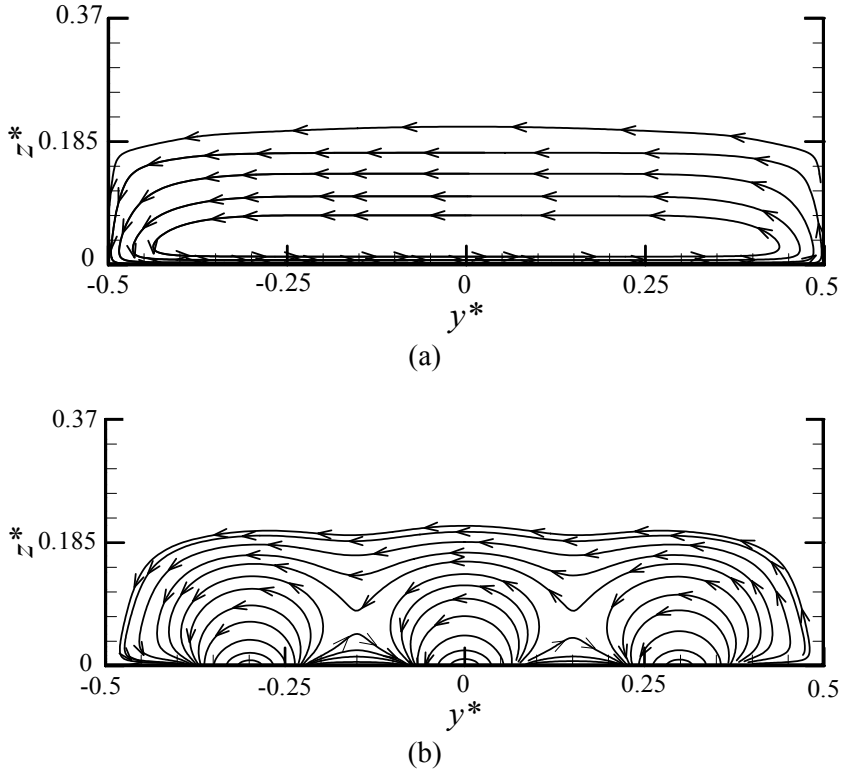

Figure 3. Electric current paths in x*=2.6 plane (Ha=30) (a) insulating wall, and (b) non-uniform electrical conductivity wall

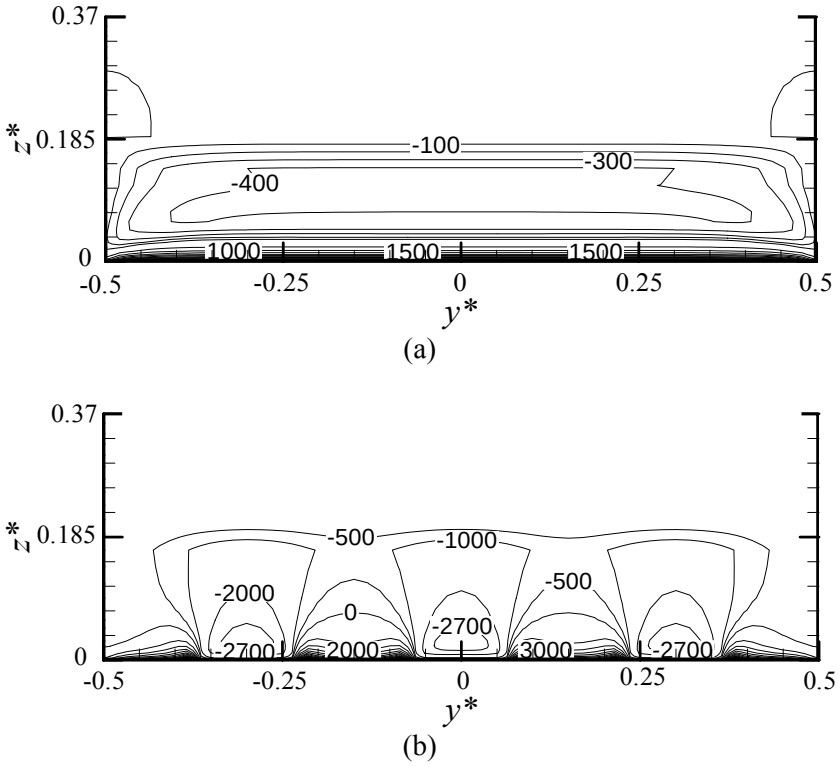

Figure 4. Lorentz force F_x distribution in x*=2.6 plane (Ha=30) (a) insulating wall, and (b) non-uniform electrical conductivity wall

The components of current which are perpendicular to the magnetic field lines generate a Lorentz-force F_x with the normal magnetic fields. Figure 4 presents the Lorentz force F_x distribution in the x*=2.6 plane for Ha=30. The negative sign in the figure indicates that the direction of the Lorentz force is opposite to the flow direction. It is obvious that the direction of the Lorentz force is inhomogeneous in different regions at the boundary layer, which is opposite to the main flow direction in the vicinity of the conducting strips but along the direction of the main flow near the insulating walls. This alternative distribution along spanwise direction of the Lorentz force may break the boundary layer, which produces intermittent perturbation on the flow near the wall, promotes the mixing of the fluid, and enhance the heat transfer.

Figure 5 depicts the velocity distribution in the x*=2.6 plane under different Hartmann numbers. The velocity distribution becomes inhomogeneous under the effect of the wall with non-uniform electrical conductivity. Obvious differences of velocity distribution appear with the increase of Hartmann numbers. The perturbation by the non-uniform electrical conductivity wall may remedy the depressing turbulent pulsations by MHD effect. The turbulent viscosity distribution in the x*=2.6 plane is depicted in Figure 6 for different Hartmann numbers. Under the effect of the non-uniform electrical conductivity wall, the turbulent viscosity exhibits a higher magnitude compared with that of an insulating wall, and displays an inhomogeneous distribution along spanwise direction. The difference of turbulent viscosity becomes more prominent with the increase of Hartmann numbers due to the greater perturbation by the non-uniform Lorentz force. Therefore, the turbulent pulsations become more furious and the ability of convective heat transfer is greatly improved.

The employment of the wall with non-uniform electrical conductivity can efficiently enhance heat transfer for free surface MHD-flow. Figure 7(a) gives local Nusselt numbers at x*=2.6 plane. The Nu/Nu0 magnitudes for all Hartmann numbers range from 1.16 to 1.65, and the enhancement effect is very obvious on the borders between the insulating walls and the conducting strips. From the results, it is evident that local Nu/Nu0 values increase as Hartmann number Ha increases in most regions because the non-uniform Lorentz force obviously modifies the velocity distribution near the bottom wall and increases turbulent pulsations with the increase of magnetic fields. Figure 7(b) shows the friction factor distribution in the x*=2.6 plane for different Hartmann numbers. It is seen that the friction factor markedly decreases as Hartmann number Ha increases in the regions of conducting strips. This is

because the Lorentz force damps the motion of the flow near the conducting strips and the velocity gradient is sharply decreased in these regions.

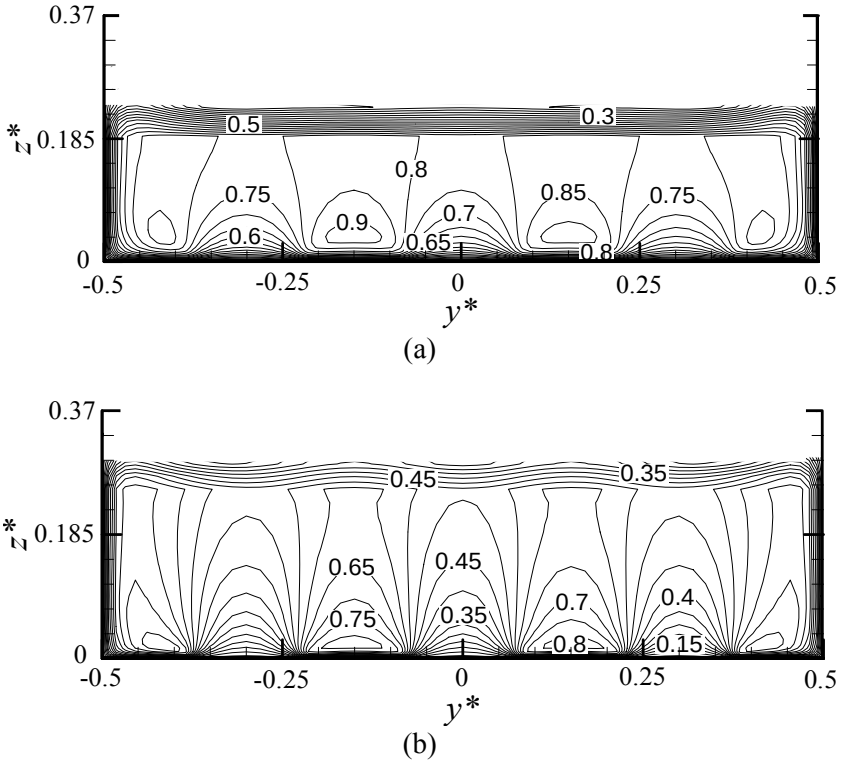

Figure 5. Velocity distribution in x*=2.6 plane, (a) Ha=30, and (b) Ha=70

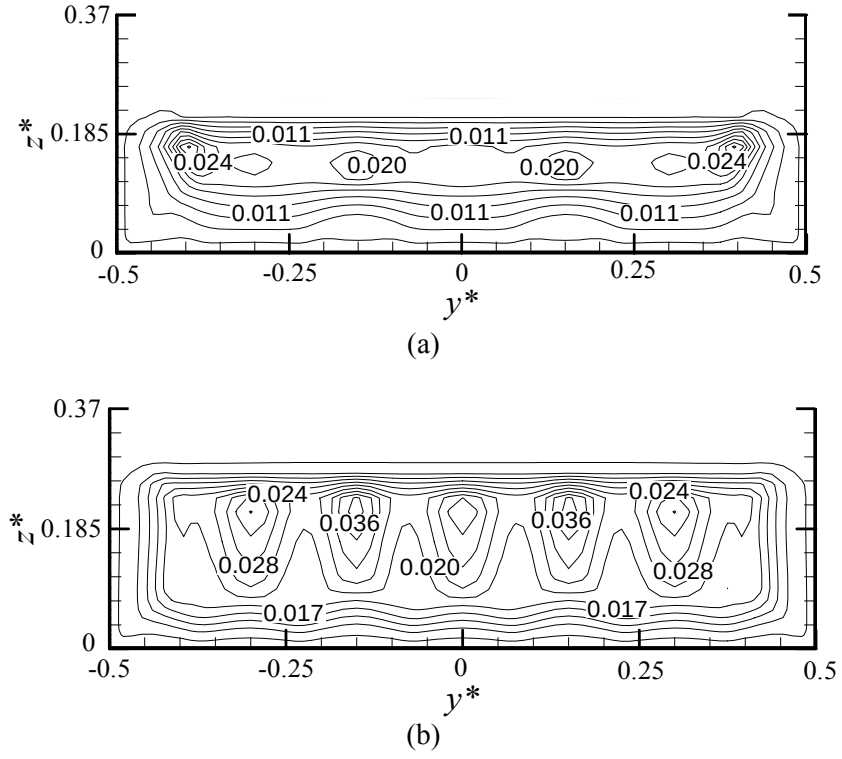

Figure 6. Turbulent viscosity distribution in the x*=2.6 plane, (a) Ha=30, and (b) Ha=70

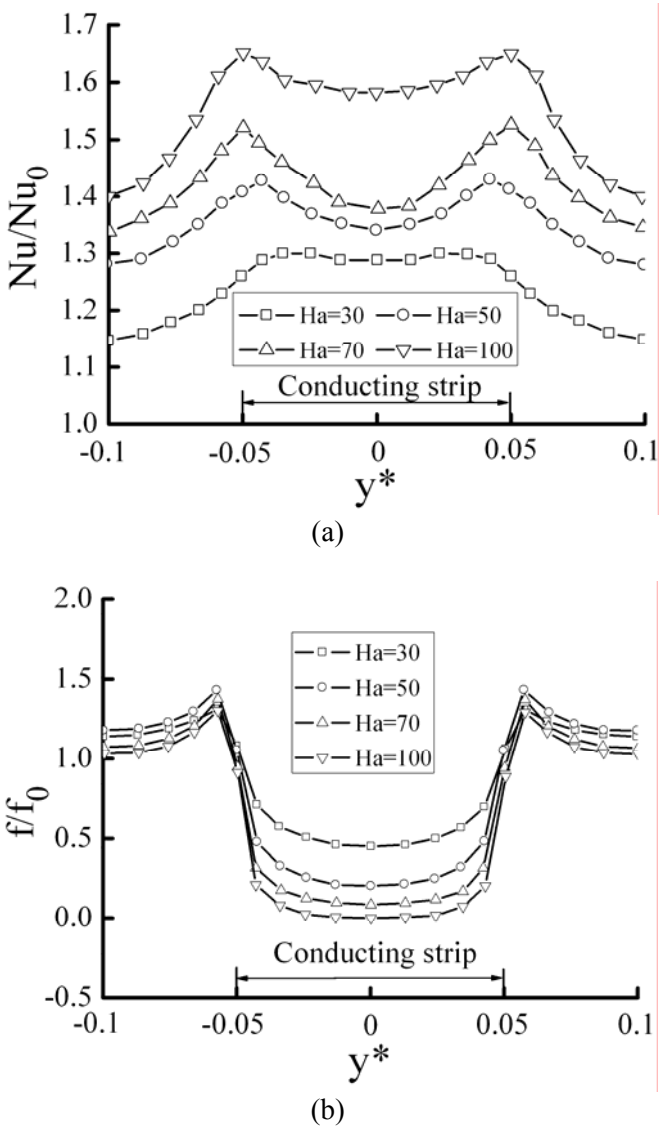

Figure 7. Distribution of Local Nu/Nu0 and Local f/f0 (At x*=2.6 plane), (a) local Nu/Nu0 at different position, and (b) local f/f0 at different position

Figure 8 illustrates the variations of the mean Nusselt number, mean friction factor and pressure drop with different Hartmann numbers. In the range of Hartmann numbers $30 \leq Ha \leq 100$, the wall with non-uniform conductivity can achieve heat transfer enhancements (Nu/Nu_0) of about 1.2 to 1.6, while the friction factors are only 0.50-0.84 relative to the insulating wall. The pressure drop increases about 1.1-1.5 relative to the insulating wall due to the increasing second flow and turbulent pulsations. In addition, heat transfer augmentation (Nu/Nu_0) is found to increase monotonically with the increase of Hartmann numbers. This curve demonstrates that the enhancement purpose for MHD-free surface flow by the way at high Hartman number is marked.

In order to investigate the heat transfer performance with different number of the conducting strips, four different models have been discussed in this paper. Table 2 shows the details of these models.

Figure 9 illustrates the variations of the mean Nusselt number, mean friction factor and pressure drop with the number of the conducting strips. It is found that the Nu/Nu_0 is influenced by the number of conducting strips, which increases first and then decreases with the increasing number of conducting strips. The friction factor ratios f/f_0 decrease with the increasing number of the conducting strips, and the pressure drop appreciably increases as the number of conducting strips increases. These curves demonstrate that the number of conducting strips has great influence on heat transfer, and the models with three or five conducting strips can achieve better enhancement effect in our research.

Table 2. Details of the models of non-uniform wall

Model number	Number of conducting strips	Width of conducting strips	Gap between conducting strips
1	m=1	0.1	/
2	m=3	0.1	0.17
3	m=5	0.1	0.075
4	m=7	0.1	0.028

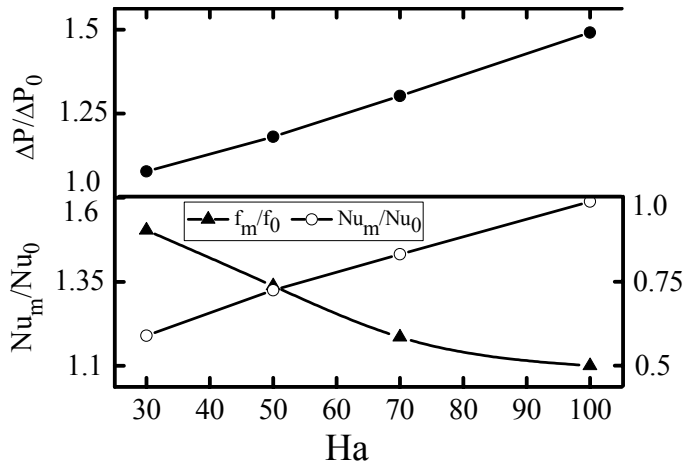

Figure 8. Distribution of the mean Nusselt number, mean friction factor and pressure drop

The performance analysis is important for the evaluation of the net energy gain to determine whether the method employed to enhance the heat transfer is effective from the view point of energy. Here, the global thermal performance ŋ = $(Nu/Nu_0)/(f/f_0)1/3$ [8] is used as the overall enhancement ratio. The results for the several cases simulated in this paper are presented in Figure 10. It is found that the thermal performance value increases with the number of conducting strips increasing up to about m=3, and starts to decrease when m >5. These curves indicate that there is an optimum strip number for heat transfer enhancement when m=3 or 5 and the maximum thermal performance values range from 1.45 to 1.95 under different Ha. In addition, the influence of magnetic fields on the thermal performance is obvious, and ŋ values increase with Hartman number increasing. Thus, the enhancement heat transfer effect for free surface MHD-flow at high Hartman number is very marked.

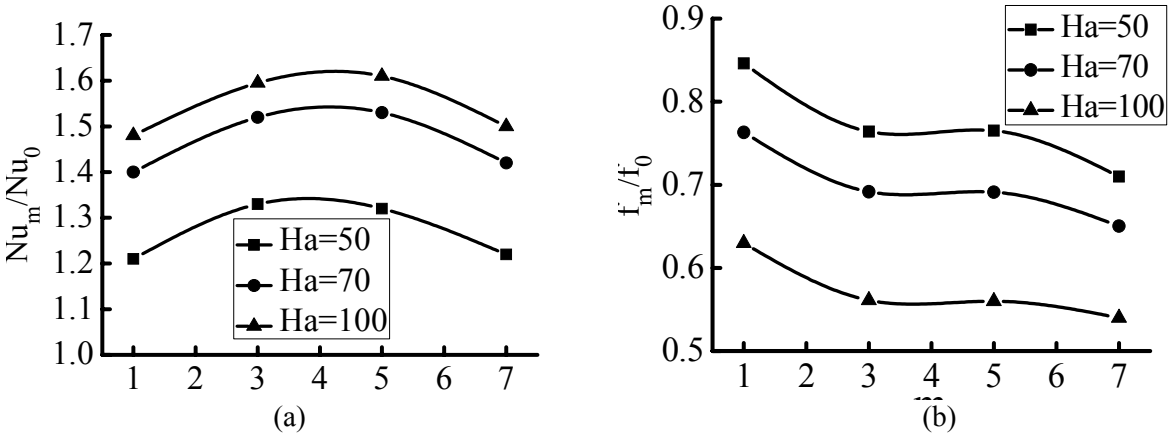

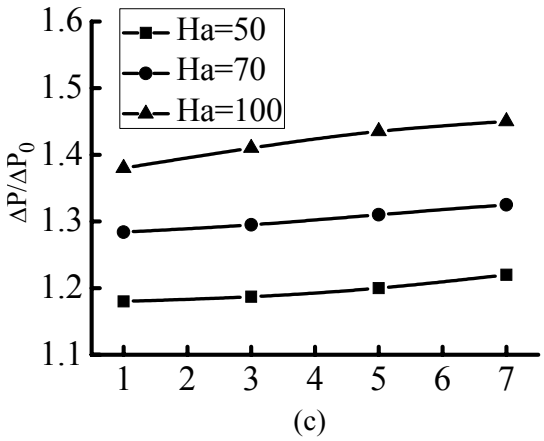

Figure 9. Distribution of the mean Nusselt number, mean friction factor and pressure drop, (a) mean Nusselt number, (b) mean friction factor, (c) pressure drop

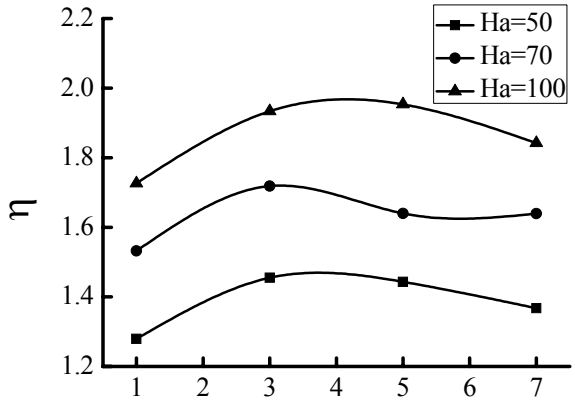

Figure 10. Global thermal performances for different model

4. Conclusions

The wall with non-uniform electrical conductivity employed in the free surface MHD-flow system to improve the heat transfer performance is performed numerically here. The conclusions are as follows:

1. The employment of the wall with non-uniform electrical conductivity can efficiently enhance heat transfer for a free surface MHD-flow, and remedy the degrading heat transfer by MHD effect.
2. In the range of Hartmann numbers $30 \le Ha \le 100$, the wall with non-uniform conductivity can achieve heat transfer enhancements (Nu/Nu_0) of about 1.2 to 1.6, while the friction loss and pressure drop are about 0.50 to 0.84 and 1.1 to 1.5 times relative to the insulating wall, respectively.
3. Heat transfer augmentation (Nu/Nu_0) increases as Hartmann number Ha increases. Therefore, the enhancement purpose at high Hartman number MHD flow is marked.
4. The number of conducting strips has great influence on heat transfer. The models with 3 or 5 conducting strips can achieve better enhancement effect in this paper.

Nomenclature

$\boldsymbol{B}$: magnetic field vector, T
$\boldsymbol{b}$: induced-magnetic-field vector, T
d: width of the channel, m
h: heat transfer coefficient, $W.m^{-2}.K^{-1}$
$\boldsymbol{J}$: current density (vector), $A.m^{-2}$
Nu: $Nu=hd/k$, Nusselt number
$\boldsymbol{B}_0$: application field vector, T
C_p: thermal capacity, $W.kg^{-1}.K^{-1}$
Fr: $Fr= U_{in}^2/gd$, Froude number
Ha: $Ha = B_0 d\sqrt{\sigma/\mu}$,Hartmann Number
N: $N=Ha^2/Re$, interaction parameter
$\boldsymbol{n}$: $\boldsymbol{n}=\nabla\phi/|\nabla\phi|$, free surface normal vector

p: pressure (N.m^{-2})
p_r: prandtl number
Re_m: $Re_m = \sigma_m \mu_m U_{in} d$, Magnetic Reynolds number
T: temperature, K
We: $We = \rho U_{in}^2 d/\sigma$, Weber number

Greece

κ: turbulent kinetic energy, m^2.s^{-2}
ε: dissipation rate of the turbulent kinetic energy
σ: surface tension, N.m^{-1}
ϕ: volume fraction
μ_m: magnetic conductivity
ρ: density of liquid metal, kg.m^{-3}
Δt: time step, s

Subscripts

e: effective
Pe: $Pe = \rho C_p U_{in} d/\lambda$, peclet number
Re: $Re = \rho U_{in} d/\mu$, Reynolds number
t: time, s
U_{in}: the velocity of inlet, m.s^{-1}
x, y, z: cartesian coordinate, m

λ: thermal conductivity, W.m^{-1}.K^{-1}
σ_m: electrical conductivity, Ω^{-1}.m^{-1}
σ_t: turbulent Prandtl number
μ: dynamic viscosity of liquid, kg.m^{-1}.s^{-1}
μ_t: the turbulent viscosity
v: velocity vector, m.s^{-1}
$\eta = (Nu/Nu_0)/(f/f_0)^{1/3}$, the global thermal performance

m: magnetic field

Acknowledgements

This work was supported by National Nature Science Foundation of China under Grand No. 50306006 and No. 50710105050.

References

[1] Kirillova, I. R., Reed, C. B., Barleon, L., Miyazaki, K. Present understanding of MHD and heat transfer phenomena for liquid metal blankets. Fusion Engineering and Design, 1995, 27, 553-569.
[2] Nygrena, R. E., Cowgilla, D. F., Ulrickson, M. A., et al. Design integration of liquid surface divertors. Fusion Engineering and Design, 2004, 72, 223–244.
[3] Buhler, L. Instabilities in quasi-two-dimensional magnetohydrodynamic flows. Journal of Fluid Mechanics, 1996, 326, 125-150.
[4] Smolentsev, S., Abdou, M., Morley, N. Application of the "k-ε" Model for Open Channel Flow in a Magnetic Field. International Journal of Engineering Science, 2002, 40, 693-711.
[5] Kitamura, K. and Hirata, M. Turbulent heat and momentum transfer for electrically conducting fluid flowing in two-dimensional channel under transverse magnetic field. 6th International Heat Transfer Conference, Toronto, 1978. Hemisphere Publishing Corp, 3, 159-164.
[6] Roache, P.J. Quantification of Uncertainty in Computational Fluid Dynamics. Annual Review of Fluid Mechanics, 1997, 29, 123-160.
[7] Dousset, V. and Pothérat, V. Numerical simulations of a cylinder wake under a strong axial magnetic field. Physics of Fluids, 2008, 20, 017104 (13).
[8] Gee D. L., Webb R. L. Forced Convection Heat Transfer in Helically Rib-Roughened Tubes. International Journal of Heat and Mass Transfer, 1980, 23, 1127–1136.

H. L. Huang Bachelor at Mechanical Engineering, Harbin University of Engineering, China at 1990. Ph.D. at Energy Engineering, University of science and Technology of China at 1996.
At present, He is full professor at Nanjing University of Aeronautics and Astronautics. He has been engaged in MHD Flows,Experimental and Numerical Heat Transfer, Applications of Solar Energy and Nuclear energy, etc., published over 50 research papers in energy and heat transfer fields. Professor Huang is the member of Association of America Physics and Association of China Energy.
E-mail address: hlhuang@nuaa.edu.cn

